the corresponding reaction products before melt processing. Evidently, the presence of GMA in the polymer reduced the degree of reordering of the clay particles during melt processing.

The XRD patterns of the reaction products before melt processing and the same materials after compression moulding, for samples containing no GMA and 1 wt% GMA, are compared in figure 4. The intensity of the reflections is proportional to the mass fraction of clay resident in agglomerates of regularly spaced clay sheets.

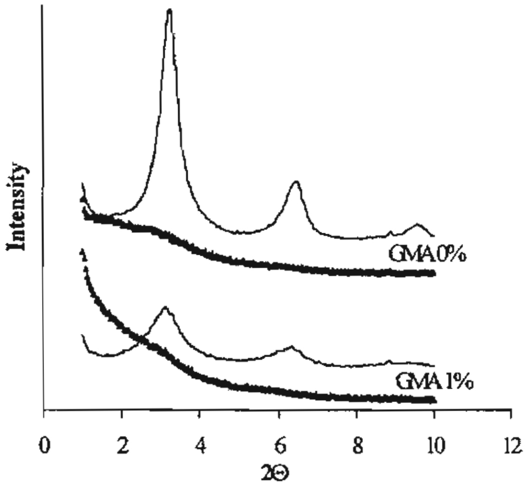

Figure 4. X-ray patterns of (Δ) the powdered reaction products and (-) the compression moulded plaques containing 50 phr of organophylic clay.

The lower peak intensities of the compression moulded sample containing GMA in comparison with the sample without GMA shows the reduced level of re-aggregation in the former sample. The GMA does not completely prevent the change, however. As detailed in part II of this work, the level of the clay dispersion may be characterised by the average aggregate thickness, L_c, and the average number layers in each aggregate, N_c.

Table 1. L_c and N_c values of the compression moulded plaques for hybrids with MMA only and the MMA / GMA sample containing 1 wt% GMA.

GMA content (wt%)	L_c (Å)	N_c
0	172	7
1	112	5

Table 1 shows that the clay aggregates in the hybrid containing 1 wt% GMA were smaller than those of hybrid containing PMMA homopolymer; i.e., the dispersion of the clay is superior in the hybrid containing GMA at the 1 wt% level.

The effects of clay content.

The poly(glycidyl methacrylate-co-methyl methacrylate) /clay hybrids were subsequently prepared with a range of organophylic clay contents; the GMA content was fixed at 1 or 10 wt% of the total monomer. The products were characterised through X-ray diffraction. The XRD traces of the reaction products and the melt processed plaques of samples containing 1 wt% GMA are shown in figure 5. The samples containing 1 wt% GMA appeared to contain delaminated clay both before melt processing for all clay contents. For organophylic clay contents of 20 and 50 phr, the reflection of the (001) plane, with d-spacings of 31.0, 27.8 Å, respectively, could be detected. Probably there is insufficient matrix polymer present to disperse the higher clay contents completely.

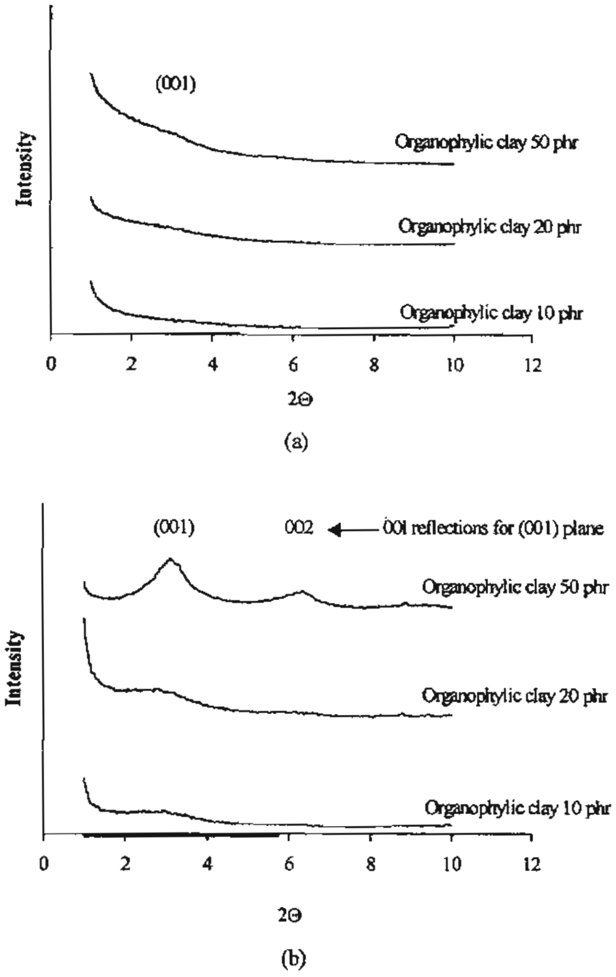

Figure 5. X-ray diffraction patterns of (a) the reaction products of the hybrids and (b) the compression moulded plaques containing 1 wt% GMA.

The L_c and N_c values for the compression moulded samples containing 1 wt% GMA are plotted as functions of clay content in figure 6. The mean clay aggregates size increases as the clay content increases. That is, the level of clay dispersion decreases for the higher clay contents. As stated previously, the quantity of polymer present at the higher filler loading is insufficient to efficiently disperse the clay.

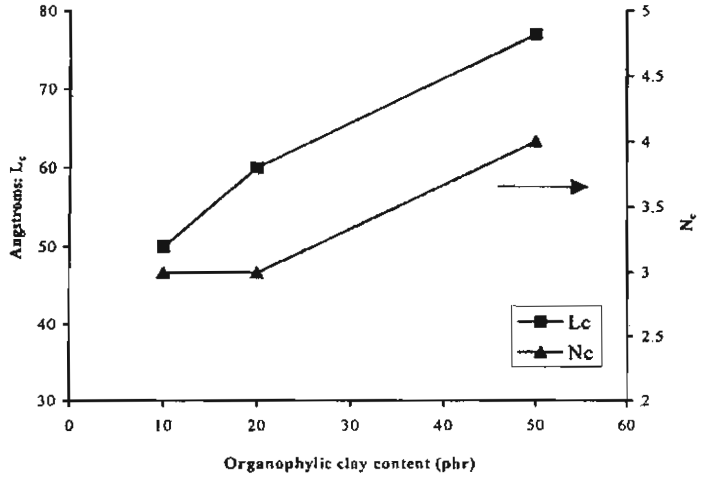

Figure 6. N_c of the compression moulded plaques containing 1 wt% GMA.

Samples containing 10 wt% GMA

The XRD traces of the hybrids and plaques containing 10 wt% GMA are shown in figure 7. Organophylic clay contents lower than 30 phr resulted in delaminated structures. Samples with clay contents of 40 and 50 phr exhibited low intensity 001 reflections for the (001) plane with corresponding d-spacings of 36.0 and 35.0 Å. After compression moulding, theses peaks became sharper.

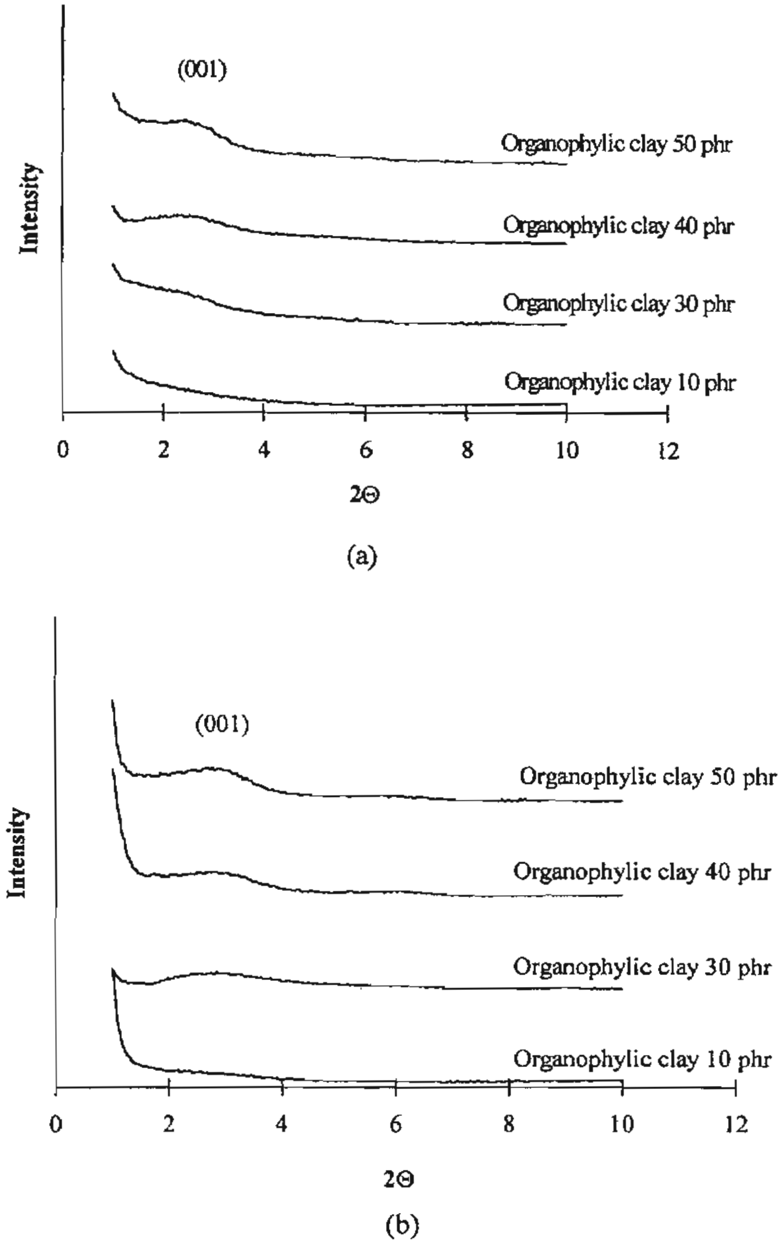

(a)

(b)

Figure 7. X-ray pattern of (a) the reaction products of the hybrids and (b) compression moulded plaques containing 10 wt% GMA.

CONCLUSIONS

The copolymerisation of MMA with GMA led to the partial stabilisation of the clay dispersion in the hybrids. However, due to the reactivity of the GMA a gelled product with an uncontrolled structure was obtained. In the subsequent work presented in part V, the GMA was replaced with maleic anhydride in attempt to maintain the thermoplasticity of matrix.

Part V

The use of maleic anhydride as a co-monomer to stabilise the clay dispersion

Abstract

Polymer / clay hybrids were prepared through the copolymerisation of methyl methacrylate and maleic anhydride. The latter was included as a functional monomer in an attempt to stabilise the clay dispersion during melt processing. It was found that maleic anhydride contents of 10 wt% in the copolymer could limit the re-aggregation of the clay. When prepared in the presence of clay, the relaxation characteristics of the copolymer were altered, probably due to the reaction of succinic anhydride groups with the amine that was bound to the organophylic clay. The product of this reaction was heterogeneous resulting in the formation of copolymer fractions with different glass-rubber transition temperatures.

Experimental

Sample preparation

Polymerisations were carried as before, except that MA was added to the reaction system. The solvent was changed from hexane to methanol due to the limited solubility of MA in hexane.

Results and discussion

Effect of MA content upon clay dispersion and stability

Samples were prepared with MA contents in the range from 1 wt% to 10 wt% of the total monomer at the constant organophylic clay content of 10 phr. The WAXD patterns of the hybrids are shown in figure 5.1. In each analysis, a small peak at from the (001) plane reflection was detected in the X-ray diffraction trace. The corresponding d-spacings of the (001) plane are 27.9, 27.9, 28.3, 28.7, and 29.4 Å, corresponding to the 0, 1, 2, 5, and 10 wt% MA content, respectively.

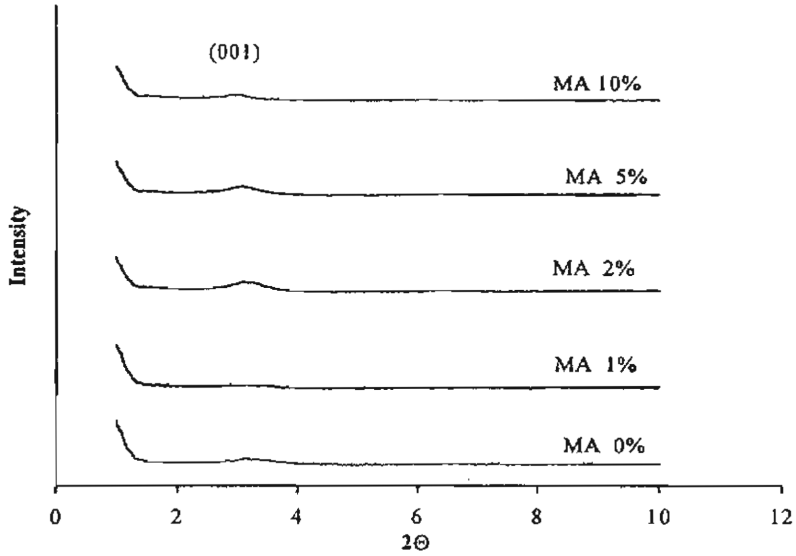

Figure 5.1 X-ray diffraction of traces of the reaction products of the poly(methyl methacrylate-co-maleic anhydride) / clay hybrids; clay content is 10 phr in each.

The clay was probably not completely delaminated in the reaction vessel since the a gel formed as the molecular weight of the polymer increased due to the limited solubility of the polymer in methanol. Figure 5.2 shows the XRD patterns of the reaction products after compression moulding. For 0, 1, 2, and 5 wt% MA contents, the XRD patterns displayed distinct reflections for the (001) plane; the corresponding d_{001} values were 28.7, 27.6, 28.1, and 27.6 Å, respectively. The sample containing 10 wt% MA had a board 001 reflection with a d_{001} of 27.6 Å. The reordering of the hybrids decreased when the MA content increased.

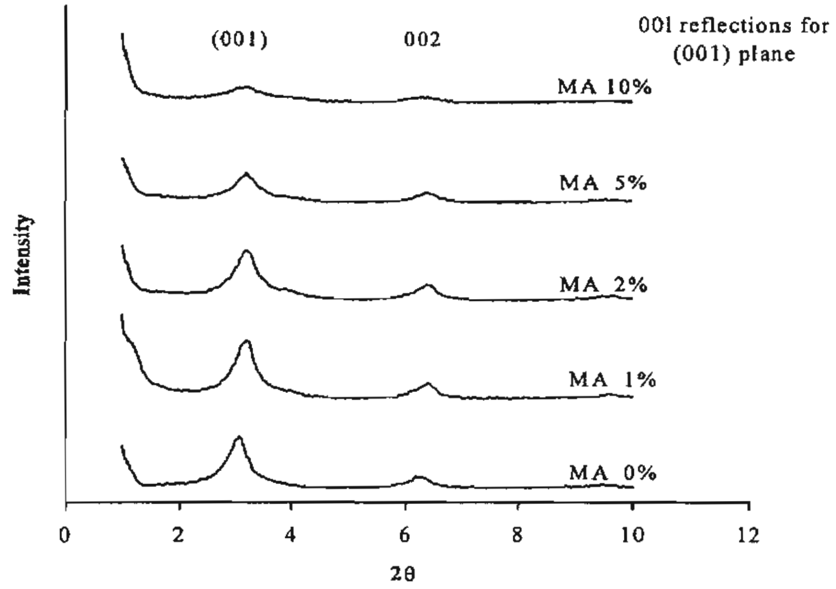

Figure 5.2 X-ray diffraction of traces of the compression moulded reaction products of the poly(methyl methacrylate-co-maleic anhydride) / clay hybrids; clay content is 10 phr in each.

The XRD patterns of the reaction products and the corresponding compression moulded plaques are compared in figure 5.3.

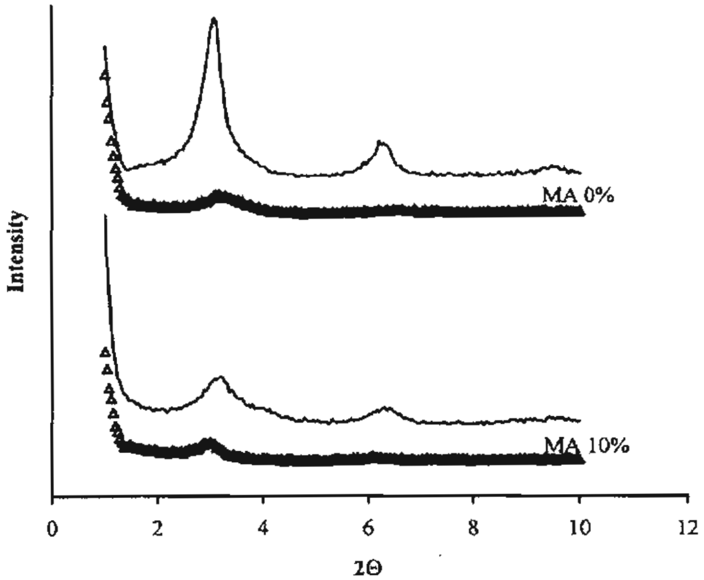

Figure 5.3 XRD traces of the poly(methyl methacrylate-co-maleic anhydride) / clay hybrids; clay content is 10 phr in each: (Δ) hybrid and (–) plaque.

Effect of clay content in the poly(maleic anhydride-co-methyl methacrylate)/clay hybrids

The copolymer containing 10 wt% was used to investigate the effect of clay content. Materials were synthesised containing organophylic clay contents in the range 10 to 50 phr. The XRD traces of the hybrids are shown in figure 5.4. The d_{001} values were 29.4, 30.7, 30.2, and 28.7 Å for 10, 20, 30, and 50 phr organophylic clay content, respectively. The 001 reflection intensity increased when the organophylic clay content increased.

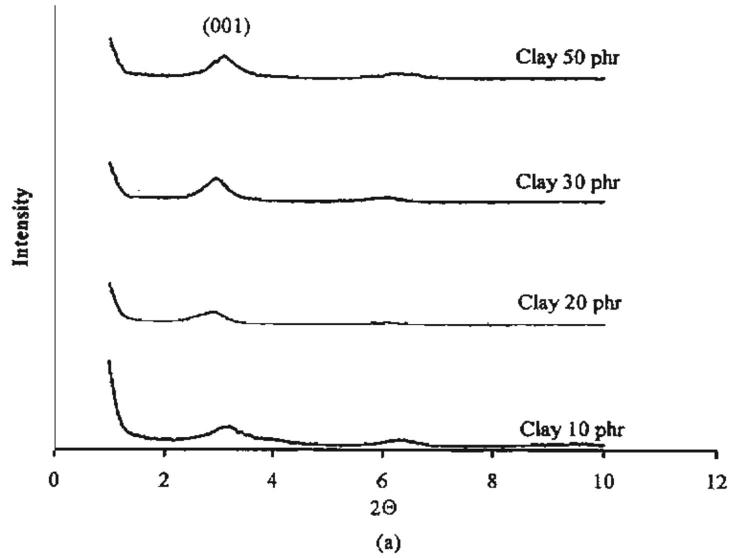

Figure 5.4 X-ray diffraction of traces of the reaction products of the poly(methyl methacrylate-co-maleic anhydride) / clay hybrids containing 10 wt% of MA.

The XRD traces of the corresponding plaques are displayed in figure 5.5. The d-spacing of the (001) plane in the plaques was 27.6, 27.9, 28.3, and 28.3 Å when the organophylic clay content was 10, 20, 30, and 50 phr, respectively. The intensity of the 001 reflection increased when the organophylic clay content increased.

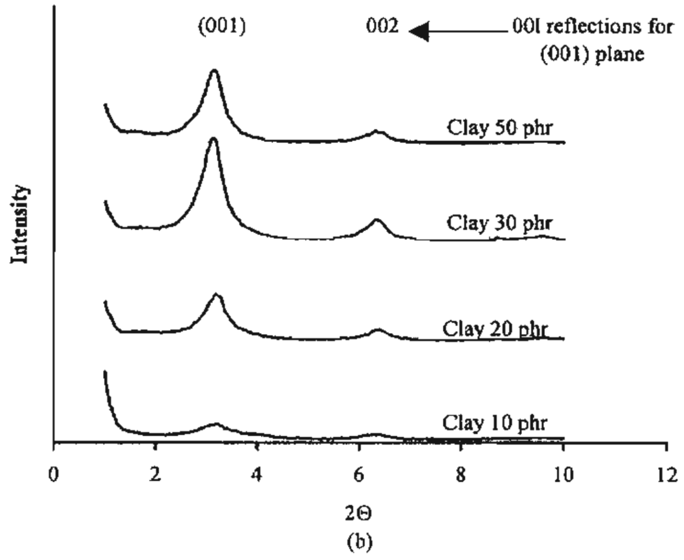

Figure 5.5 X-ray diffraction of traces of the compression moulded poly(methyl methacrylate-co-maleic anhydride) / clay hybrids containing 10 wt% of MA.

The Scherrer crystal thickness values, L_c, calculated from the 001 reflection of the moulded poly(methyl methacrylate-co-maleic anhydride) / clay hybrids plaques are shown in table 5.1; these data are plotted in figure 5.6. The FWHM decreased when the organophylic clay content increased and therefore L_c increased.

Table 5.1 L_c values associated with the (001) plane for the plaques containing 10 wt% MA.

The organophylic clay content (phr)	FWHM (°2θ)	L_c (Å)
10	0.639	138
20	0.501	177
30	0.485	182
50	0.461	192

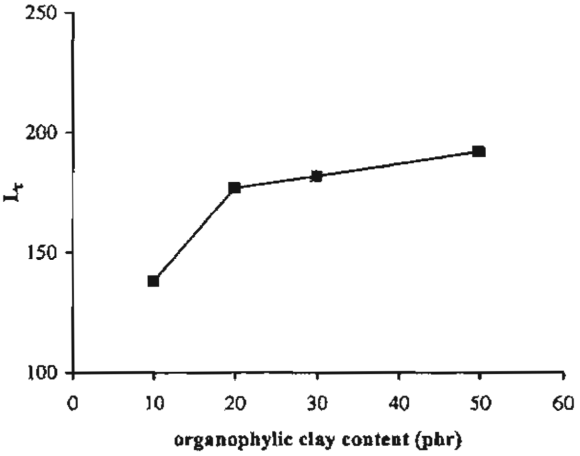

Figure 5.6 Scherrer crystal thickness, L_c, from peak width of 001 reflection of the moulded poly(methyl methacrylate-co-maleic anhydride) / clay hybrids containing 10 wt% MA.

Relaxation characteristics

The relaxation characteristics of the compression moulded poly(methyl methacrylate-co-maleic anhydride) containing 10 wt% of MA were determined through DMA; the data are plotted in 5.7.

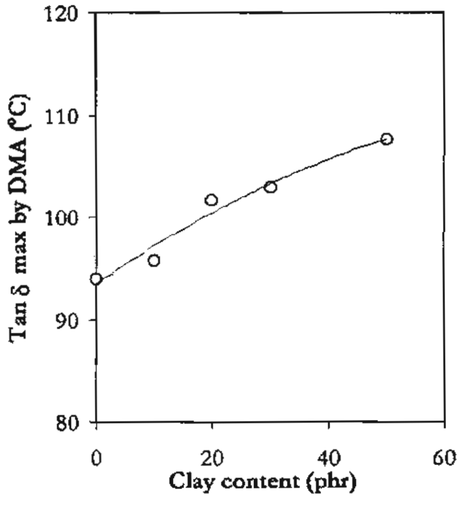

Figure 5.7 Relaxation temperatures, by DMA, of the compression poly(methyl methacrylate-co-maleic anhydride) containing 10 wt% MA.

Apparently, the temperature of the main relaxation event is a function of the clay content. To investigate this further, the poly(methyl methacrylate-co-maleic anhydride) copolymers containing 10 wt% of MA were extracted from the reaction products and the compression moulded hybrids; the extracts were characterised through DSC. The thermograms had two relaxation events, indicating a heterogeneous structure of the copolymer. The temperatures of these relaxations are plotted as functions of clay content in figure 5.8.

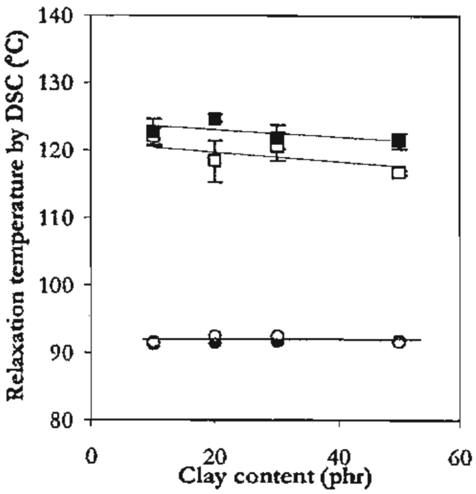

Figure 5.8 Relaxation temperatures, by DSC, of the poly(methyl methacrylate-co-maleic anhydride) containing 10 wt% MA: extracted from mouldings (1st transition ●, 2nd transition ■) and (1st transition O, 2nd transition □) of the reaction products.

The differences in relaxation characteristics must be related to changes in polymer microstructure. ^{1}H-NMR analysis revealed that the copolymer extracted from the composites containing higher clay contents had an additional resonance at 6.7 ppm that was not detected in the copolymer prepared in the absence of clay. This resonance may be due to the presence of amide resulting from the reaction of MA with the amine that was used to modify the clay. It is possible that the structure produced as a consequence of this reaction has a higher Tg than the poly(methyl methacrylate-co-maleic anhydride). The two relaxation events seen in the DSC analysis suggest that the solvent extraction process resulted in the fractionation of the polymer due to solubility differences of components. It is speculated that the copolymer in close proximity to the clay reacts to a greater extent with the amine than copolymer in the bulk, the former creating a higher Tg fraction and the latter a lower Tg fraction. The dependence of Tg by DMA upon clay content implies that the copolymer fractions were at least partially mixed in the melt-pressed plaques. The relaxation events observed around 120° C, by DSC, of the copolymer extracted from the reaction products were approximately 5°C lower than the corresponding events in the copolymers that were extracted from the compression mouldings. This may be the result of the further reaction of the MA in the copolymer upon pressing to form the plaques. Further characterisation tests are needed to clarify these details.

Conclusions

The presence of MA in the copolymer led to enhanced stability of the clay dispersion of the moulded samples. The reactivity of the anhydride groups caused microstructure changes in the polymer that resulted in changes in the relaxation characteristics of the polymers. The details of the process must be clarified, and quantified, through further analysis of the characterisation data.

Out put from the PROJECT
International journal

1. Tabtiang, A., Lumlong, S., and Venables, R. A., *'The influence of preparation method upon the thermomechanical characteristics of poly(methyl methacrylate) / clay composites'*, ***Eur. Polym. J.***, **36**(12), pp. 2559-2568 (2000)
2. Tabtiang, A., Lumlong, S., and Venables, R. A., *'The effects of shear and thermal history upon the microstructure of solution polymerised poly(methyl methacrylate) / clay composites'*, ***Polym.-Plast. Technol. Eng.***, **39**(2), pp. 293-303 (2000)
3. Tabtiang, A. and Venables, R. A., *'The stabilisation of the clay dispersion in poly(methyl methacrylate) / clay hybrids through the use of functional co-monomers'*, in preparation.

POLYMER-PLASTICS TECHNOLOGY AND ENGINEERING

Editor: MUNMAYA K. MISHRA

POLYM.–PLAST. TECHNOL. ENG., 39(2), 293–303 (2000)

EFFECTS OF SHEAR AND THERMAL HISTORY ON THE MICROSTRUCTURE OF SOLUTION POLYMERIZED POLY(METHYL METHACRYLATE)–CLAY COMPOSITES

A. TABTIANG, S. LUMLONG, and
R. A. VENABLES*

Department of Chemistry
Faculty of Science
Mahidol University
Rama VI Road
Bangkok, 10400, Thailand

Abstract

Poly(methyl methacrylate)–clay composites were synthesized through free-radical solution polymerization of methyl methacrylate in the presence of clay that was preintercalated with dodecylammonium or hexadecyltrimethylammonium ions. Neither the diffraction peak from the (001) plane nor the 00*l* reflections for the (001) plane were observed during x-ray characterization, showing that the clay particles were greatly expanded (i.e., exfoliated) in the reaction products, due to the presence of large quantities of polymer between the clay layers. Syntheses carried out with high clay loadings resulted in reductions in the weight and number-average molecular weights and increases in the polydispersities of the polymers, caused by chain transfer to active sites on the surface of the clay. It was found that heat and shear, during subsequent processing of the reaction products, resulted in reordering of the microstructure through narrowing of the clay galleries with the partial exclusion of the polymer. The final interlayer spacings were determined by the orienta-

---

* To whom correspondence should be sent.

www.dekker.com

tion and lengths of the preintercalated alkylammonium ions. It was concluded that the exfoliated structure created during polymerization was unstable under the processing conditions and, consequently, reordered into a more stable form.

Key Words: Poly(methyl methacrylate); Clay; Composite; Hybrid.

INTRODUCTION

Polymer–clay composites with fine dispersions of reinforcing particles may be prepared by using the swelling properties of smectite clays (1), whereby a polar molecule intercalates the clay layers and, consequently, increases the interlayer spacing. This process may be carried out in several steps, the essential features of which are the following: (1) exchange of the clay's sodium ions with alkylammonium ions to partially expand the clay galleries and to reduce the hydrophilicity of the clay's surface, yielding a modified clay; (2) swelling of the modified clay with monomer; and (3) polymerization of the monomer. An example of this type of system is the polyimide–clay hybrid described by Yano et al. (2), where a film containing montmorillonite clay was synthesized from a dimethylacetamide solution of poly(amic acid) and a dimethylacetamide dispersion of montmorillonite, intercalated with an ammonium salt of dodecylamine. The final product showed improved barrier properties to the permeation of vapors, in comparison with the unmodified polyimide. Other systems have shown improved mechanical properties at elevated temperatures (3).

Although poly(vinyl chloride) (PVC) is a low-cost material with versatile properties, its performance is limited in some applications where elevated temperatures are experienced, due to its low softening temperature. Properties may be improved, however, by blending the PVC with engineering resins that possess high glass transition temperatures (T_g). These resins have been referred to as HT additives (4). Examples include those based on poly(methyl methacrylate) (PMMA), styrene–maleic anhydride copolymer, and brominated polycarbonate. The HT additive should be miscible or partially miscible with the PVC to maintain optical clarity. Because of the outstanding heat distortion temperature properties of polymer–clay hybrids (3), a hybrid may perform suitably as a HT additive for PVC. Thus, in this work, an additive of this type was prepared through solution polymerization of methyl methacrylate in the presence of modified clays, for use in rigid PVC formulations. PMMA was chosen because of its known compatibility with PVC (5) and inherently high T_g. The PMMA is intended to act as a carrier polymer to bring the dispersed clay layers into the PVC matrix. The objectives of the work described herein were to establish the initial structure of the additive and, because it will experience heat and hydrodynamic stresses during processing, to determine the processing effects on the final structure.

EXPERIMENT

Materials

The inhibitor was extracted from methyl methacrylate (MMA) (Fluka) with $NaOH_{(aq)}$, then washed with distilled water, and subsequently dried over anhydrous Na_2SO_4. Bentonite clay, containing a minimum of 90% montmorillonite, was from Colloid Environmental Technologies Co., Ltd. Dodecylamine was from Fluka, hexadecyltrimethylammonium chloride from Merck, and 2,2′-azo-bis(isobutyric-nitrile) (AIBN) initiator was supplied by TPI Co., Ltd., Thailand.

Synthesis of Modified Clay

Clay (20 g) was dispersed in distilled water (600 mL) at 80°C. To this was added a solution of dodecylamine or hexadecyltrimethylammonium chloride (0.05 mol) and concentrated hydrochloric acid (4.8 mL) in distilled water (100 mL). Heating and stirring was continued for 1 h while maintaining the temperature at 80°C. The suspension was then filtered and the solid residue washed with hot distilled water until no chloride was left, as determined by using the silver nitrate test. The product was dried at 60°C for several days in a fan oven, then milled in a ball mill, and subsequently dried at 60°C under vacuum for 24 h, yielding the dodecylammonium–clay (DDA–clay) and hexadecyltrimethylammonium–clay (HDA–clay).

Composite Preparation

2,2′-Azo-bis(isobutyric-nitrile) (0.1 g) was dissolved in the extracted MMA (10 g), followed by the addition of the modified clay (1, 2, 5, or 10 g) and distilled hexane (40 mL). For the highest clay contents, 100 mL of hexane was needed to disperse the clay. The reaction flask was suspended in a thermostated water bath at 68°C for 5 h, with a condenser fitted. The powdered product was recovered from the reaction mixture by evaporation of the solvent, followed by drying under vacuum at 60°C. Portions of the products were either melt fluxed in a Haake Rheocord 90 at 180°C for 5 min, with a rotor speed of 50 rpm, to give the samples a melt processing history, or statically annealed in a fan oven for 30 min at 175°C. All melt-fluxed samples were compression molded at 180°C to form plaques for characterization.

Characterization

Wide-angle x-ray diffraction (WAXD) measurements were carried out using a JEOL JDX-3530. The Cu K_α radiation source was operated at 30 kV and 30 mA. The scanning speed, step angle, and count time were 1.2°2θ/min, 0.04°2θ, and 2 s, respectively. For the scan range 1–10°2θ, the divergence slit, receiving slit, and scattering slit were 0.5°, 0.1 mm, and 0.5°, respectively, whereas for the range 3–40°2θ, these values were 1°, 0.2 mm, and 1°, respectively. Infrared data were collected using a Perkin Elmer FT2000 and diffuse reflectance (DRIFT) accessory. Gel permeation chromatography (GPC) was carried out on the polymer extracted from the composites with tetrahydrofuran at room temperature, using a Waters 150-CV Plus. Thermogravimetric analyses (TGA) were carried out using a Perkin Elmer TGA7.

RESULTS AND DISCUSSION

Characterization of Modified Clay

Figure 1 shows DRIFT spectra of the unmodified clay and DDA–clay. The presence of protonated dodecylamine in the clay galleries is shown by the

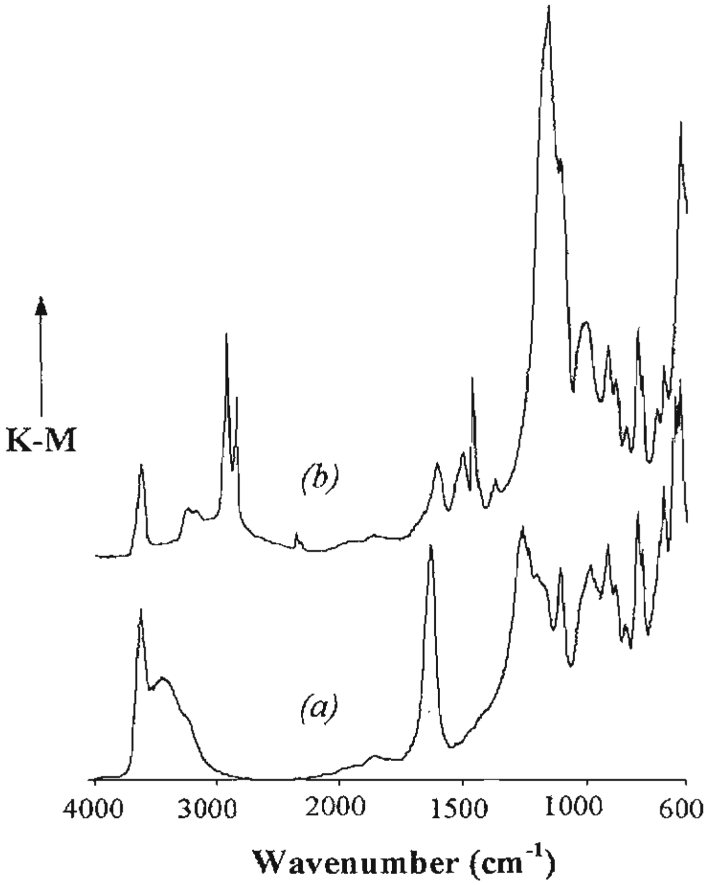

FIG. 1. DRIFT spectra of (a) unmodified clay and (b) DDA–clay.

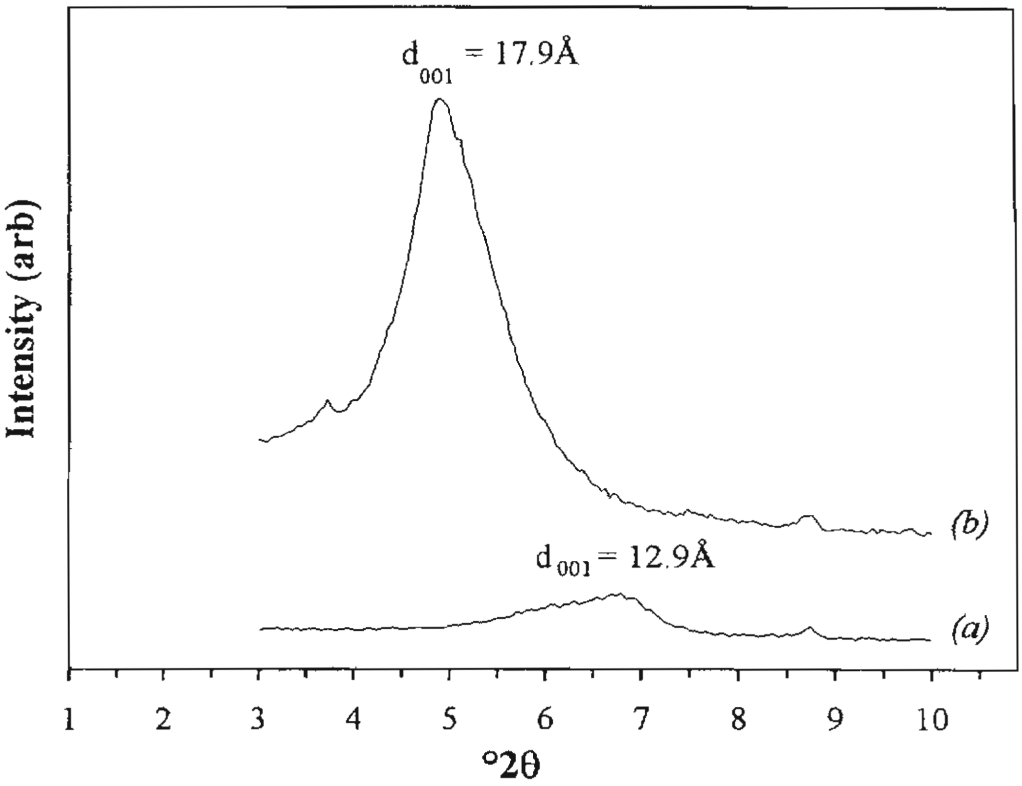

FIG. 2. X-ray diffraction traces of (a) unmodified clay and (b) DDA–clay.

N—H stretching of the NH_3^+ group in the region 3260–3181 cm^{-1} and the CH stretching peaks in the range 2925–2852 cm^{-1}. The O—H stretching bands at 3400–3200 cm^{-1} and the HOH bending peak at 1641 cm^{-1} of adsorbed interlayer water (6) found in the original clay were absent in the modified sample, because of the reduced hydrophilicity of the internal surfaces of the clay. The average quantity of intercalated dodecylammonium ions, from four replicated TGA analyses of the modified clay, was 17.7 wt%. The x-ray diffraction patterns of the unmodified and modified clays are displayed in Fig. 2. The *d*-spacing of the (001) plane, d_{001}, in the original clay was 12.9 Å, whereas that of the DDA–clay was 17.9 Å. The gallery spacing (i.e., the distance between the internal surfaces of neighboring clay layers) is calculated from the difference between d_{001} and the van der Waal's thickness of the clay layer. This thickness is estimated at 9.6 Å (7). For the DDA–clay, the gallery spacing was $17.9 - 9.6 = 8.3$ Å. This gallery spacing is too small to accommodate the dodecylammonium ions standing perpendicular to the surface of the clay, as the total length of the extended ion is around 20 Å (7). The more probable orientation is that one molecule lies parallel to each of the internal surfaces of the clay, in a bilayer orientation (8). Similar results were obtained for HDA–clay.

Characterization of Polymerization Products

In the x-ray traces of the reaction products from solution polymerization containing DDA–clay, neither peaks from the montmorillonite's (001) plane nor the 00*l* reflections for the (001) plane were seen in the range 1–10°2θ. The absence of the (001) diffraction peak shows that during polymerization, d_{001} increased to a distance greater than that measurable with the minimum scan angle of the powder diffractometer (i.e., greater than around 88 Å). This may be considered an exfoliated arrangement of the clay layers (9). In the x-ray trace for the PMMA without clay, an increase in intensity at low angles was observed that was caused by the primary beam contribution to the signal. For the clay-containing samples, the onset of a very broad scattering signal, from the (001) plane, associated with the clay sheets at distant irregular spacings was superimposed on the primary beam signal. The original structure of the modified clay is largely destroyed, however.

The dispersion force, dipole–dipole interaction, and hydrogen-bonding contributions to the solubility parameter (10) of MMA are around 15.7, 8.2, and 6.7 $(\mathrm{MPa})^{1/2}$, respectively, compared to the corresponding values of 16.7, 0.0, and 0.0 $(\mathrm{MPa})^{1/2}$, respectively, for hexane, and hence the MMA monomer will tend to displace the hexane from the clay galleries, due to its more favorable specific interactions with the surface of the clay, causing the clay to swell. The gain in freedom of the dodecylammonium ions and hexane molecules as the interlayer spaces enlarge counterbalances the loss in entropy of the monomer. As the polymer precipitates from the solution, it is trapped in the interlayer, thereby fixing the distant separation of the clay sheets. The quantity of clay present during polymerization did not affect the extent of clay delamination.

Gel permeation chromatography data showed that DDA–clay contents up to 7 vol% did not significantly affect the molecular weight or the polydispersity. Clay contents of 15 vol% or more caused reductions in molecular weight and increased polydispersity. When the ratio of clay to monomer is high, chain transfer to the clay due to interactions with Brönsted sites on the clay's surface may become significant, with consequent alterations to the molecular-weight parameters. This may be related to the larger quantities of solvent that were required during synthesis in the presence of high clay contents, resulting in more dilute reaction conditions. Chain transfer to the solvent itself may not be the predominant mechanism, however, because *n*-hexane cannot form sufficiently stable radical intermediates (11).

Effects of Shear and Thermal History

X-ray traces of the melt-processed polymerization products containing DDA–clay are shown in Fig. 3. It is apparent that the (001) diffraction, fol-

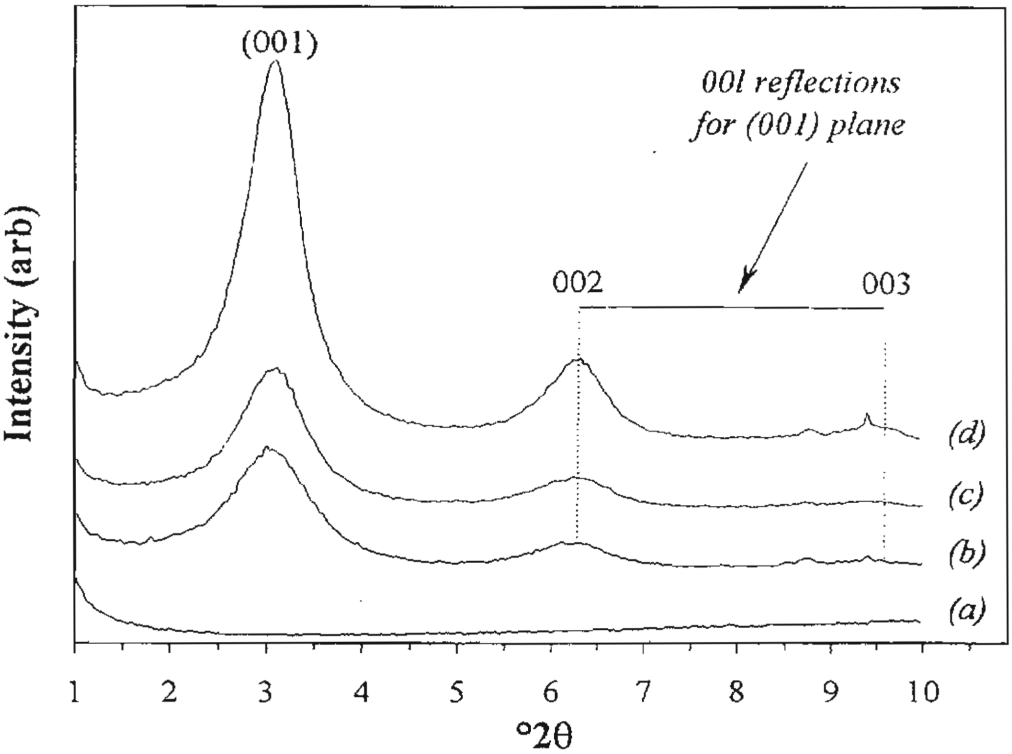

FIG. 3. X-ray diffraction traces of (a) PMMA without clay and the melt-processed DDA–clay composites containing (b) 10, (c) 20, and (d) 50 phr of clay.

lowed by two less intense signals with regular displacement along the °2θ axis, is present. The less intense signals are the 00*l* reflections for the (001) plane; the corresponding *d*-spacing is around 29 Å. Thus, at least some of the clay layers change from the expanded arrangement that is created during solution polymerization to a closer-packed configuration after melt processing. Moreover, the resultant d_{001} changes little with increasing clay content.

To assess the effect of heat alone without the concurrent application of pressure and stress, the powdered reaction products were statically annealed. The presence of the 00*l* reflections for the (001) plane implied that some thermally induced reordering of the clay layers occurs upon static annealing. The peaks were less intense than in the melt-fluxed samples, showing that the extent of reordering was lower. This difference may simply be kinetic in origin, whereby the mechanical work during mixing greatly accelerates the system toward the thermodynamic equilibrium position. The structural changes may also be influenced by the melt-elasticity contribution to the free energy of the system, however. This is analogous to the situation in partially miscible blends where the temperatures of phase dissolution or separation are altered under shear; both enhanced and reduced miscibility has been observed (12). The absence of the (100) peak, at °2θ = 19.5, in the melt-processed sample shows that during compression molding, the silicate sheets move under pressure to lie parallel to the mold surface. In the powdered reaction products, the clay is randomly oriented; hence, the (100) plane is detected.

At the processing temperature, the specific interactions between the PMMA and the clay surface become weakened by the increased thermal motion of the molecules. The clay particles rearrange to a more thermodynamically stable state. This occurs through the expulsion of some of the PMMA chains from between the silicate sheets, allowing the layers to approach one another more closely. The driving force may be the gain in entropy of the polymer chains as they are freed from their confinement. The d_{001} values in the melt-processed DDA–clay composites were typically around 29 Å, giving an interlayer spacing of 19.4 Å. The length of the extended dodecylammonium ion is estimated to be 20.2 Å (7); that is, its length is approximately the same as the gallery spacing. This suggests that the gallery ions adopt a near-perpendicular orientation to the clay sheets in the presence of the PMMA melt and span the gallery from one clay layer to the next, thereby partially controlling the interlayer distance. This phenomenon was investigated further by using HDA–clay, containing the longer alkylammonium ion, to prepare the composites. The x-ray data for these materials show that the polymerization products (Fig. 4a) similarly contained greatly expanded clay, inferred from the absence of the (001) peak and the 00*l* reflections from the (001) plane. The statically annealed and melt-processed HDA–clay composites (Figs. 4b and 4c, respectively) both show series of 00*l* reflections, which correspond to a d_{001} of 38.8 Å and gallery spacing of 29.2 Å. The extended chain length of the hexadecyltrimethylammonium ion is around 29 Å; hence, it is reasonable to infer that the aliphatic chains of the ion are oriented perpendicular to the surface of the clay and, therefore, control the gallery spacing. This indicates that the same reordering of the dispersed clay layers occurs for both of the modified clays.

The d_{001} in the melt-processed composites can be explained qualitatively through consideration of the thermodynamic forces that drive the system (13,14). The gallery spacing is restricted through the loss in entropy due to the confinement of the polymer and by any unfavorable pairways interactions among the clay surface, polymer, and alkylammonium ions. It is driven to expand through the gain in entropy of the alkylammonium chains and the exothermic interactions between the clay and PMMA. Upon melt fluxing, the distance between the clay layers reduces, as the PMMA chains move out from between the clay layers to gain entropy, until the distance that is equal to the length of the extended alkylammonium ions is reached. At this point, the con-

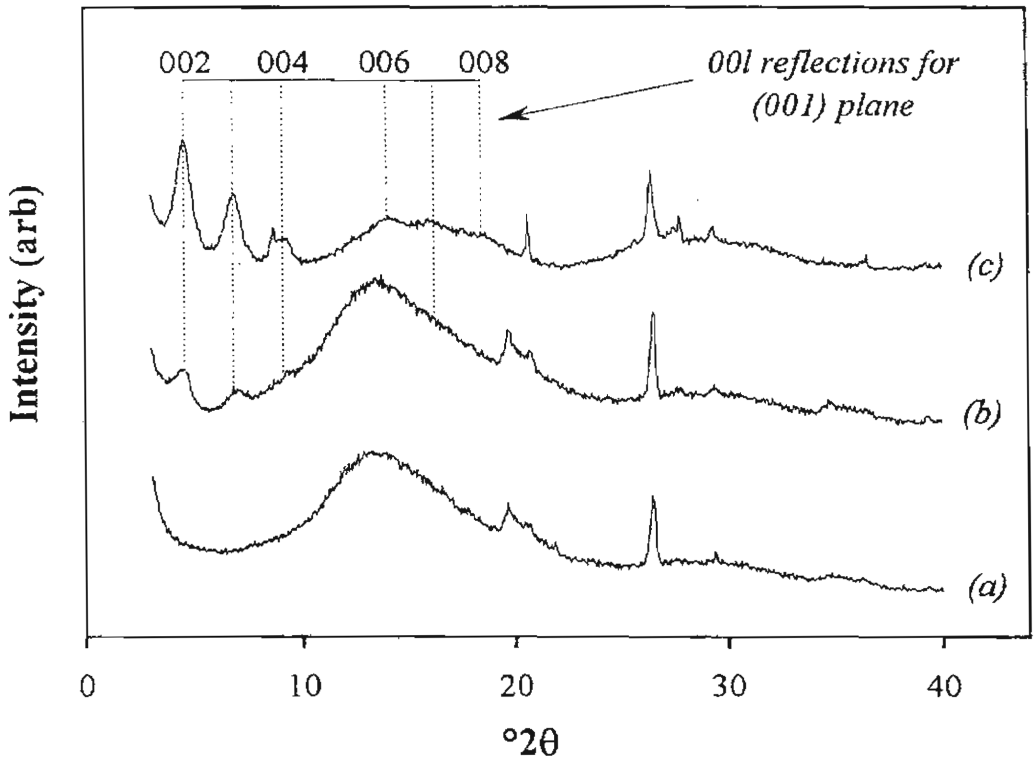

FIG. 4. X-ray diffraction traces of HDA–clay composites: (a) powder reaction product; (b) reaction product after static annealing; (c) the reaction product after melt processing.

traction is arrested, because further narrowing of the galleries would result in the unfavorable loss in entropy of the alkylammonium ions. The final gallery spacing is therefore approximately the same as the length of the alkylammonium ions. The heat of polymer–clay interaction under these conditions is sufficient to overcome the loss in entropy of the remaining confined polymer. Hence, some of the PMMA remains in the galleries, causing the alkylammonium ions to maintain their perpendicular orientation.

In the transmission electron micrograph of a melt-processed DDA–clay composite, shown in Fig. 5, it can be seen that the silicate sheets are present in aggregates of three to five primary layers; the distances between these aggregates are around 85 Å. Moreover, in the top region of the image, an isolated sheet can be seen. The x-ray analysis described earlier responds to the structure within the aggregates, showing that the interlayer distance within the aggregates is small and is typically 19.4 Å. These observations show that the clay layers are still partially delaminated after melt processing.

FIG. 5. Transmission electron micrograph of DDA–clay aggregates in a melt-processed sample.

CONCLUSIONS

1. Solution polymerization of MMA in hexane, in the presence of DDA–clay and HDA–clay, produces PMMA–clay composites containing silicate sheets that are exfoliated to a separation beyond the detection limit of the x-ray analysis.
2. Free-radical polymerizations in the presence of high clay loadings result in reductions in the weight and number-average molecular weights and increases in the polydispersity of PMMA.
3. The exfoliated structure is unstable under processing conditions and, consequently, reordering of the clay particles, through narrowing of the clay galleries with the exclusion of some of the polymer, takes place. The final clay structure is partially delaminated and comprises small aggregates of sheets, separated by distances of around 85 Å. The interlayer spacing within the aggregates is considerably smaller and is controlled by the orientation and length of the extended preintercalated alkylammonium ions.

ACKNOWLEDGMENTS

The authors would like to thank the Thailand Research Fund (TRF), for their support of this work, the National Metal and Materials Technology Centre

(MTEC) for the use of the x-ray diffractometer and TGA, to Naowarath Manomaisantiphap for some of the x-ray analyses, and to Dr. Nopadol Chaikum for helpful discussions.

REFERENCES

1. W. E. Worral, *Clays and Ceramic Raw Materials,* Applied Science Publishers, London, 1975.
2. K. Yano, A. Usuki, and A. Okada, *J. Polym. Sci. A: Polym. Chem., 35,* 2289 (1997).
3. A. Usuki, A. Koiwai, Y. Kojima, M. Kawasumi, A. Okada, T. Kurauchi, and O. Kamigaito, *J. Appl. Polym. Sci., 55,* 119 (1995).
4. K. Marossy and L. E. Tarjanyi, *Conference Proceedings of "PVC '93,"* Institute of Materials, PVC Group of the Polymer Industry Division, Brighton, U.K., 1993, p. 225.
5. R. Flores, J. Perez, P. Cassagnau, A. Michel, and J. Y. Cavaillé, *J. Appl. Polym. Sci., 60,* 1439 (1996).
6. S. W. Webb, D. A. Stanley, and B. J. Scheiner, *Bureau of Mines Report of Investigations RI9036,* U.S., Department of the Interior, Bureau of Mines, Washington, DC, 1986.
7. T. Lan, K. D. Kaviratna, and T. J. Pinnavaia, *Chem. Mater., 7,* 2144 (1995).
8. M. Ogawa and K. Kuroda, *Bull. Chem. Soc. Jpn., 70,* 2593 (1997).
9. E. P. Giannelis, *Adv. Mater., 8*(1), 29 (1996).
10. J. A. Brydson, *Plastics Materials Sixth Edition,* Butterworth-Heinemann, Oxford, 1995, pp. 81–82.
11. J. M. G. Cowie, *Polymers: Chemistry and Physics of Modern Materials,* Blackie Academic and Professional, London, 1991, pp. 64–65.
12. H. W. Kammer, C. Kummerloewe, J. Kressler, and J. P. Melior, *Polymer, 32*(8), 1488 (1991).
13. R. A. Vaia and E. P. Giannelis, *Macromolecules, 30,* 7990 (1997).
14. R. A. Vaia and E. P. Giannelis, *Macromolecules, 30,* 8000 (1997).

ELSEVIER SCIENCE Ltd. [DTD 4.1.0]
JOURNAL EPJ ARTICLE No. 1754
PAGES 1-10 DISPATCH 23 March 2000
EPJ 1754
PROD. TYPE: FROM DISK
A

ELSEVIER
European Polymer Journal 000 (2000) 000–000
EUROPEAN POLYMER JOURNAL

The influence of preparation method upon the structure and relaxation characteristics of poly(methyl methacrylate)/clay composites

Arunee Tabtiang, Saisamorn Lumlong, Richard A. Venables *

Department of Chemistry, Faculty of Science, Mahidol University, Rama VI road, Bangkok, 10400, Thailand

Received 15 October 1999; accepted 14 February 2000

Abstract

Poly(methyl methacrylate) (PMMA)/clay composites were prepared using two methods: through solution polymerisation of methyl methacrylate in the presence of alkylammonium-modified clay and through the direct melt intercalation of PMMA. Both composites were fluxed in an internal mixer to give comparable melt processing histories. In the reaction product of the polymerisation method, the clay layers were separated to a distance greater than 80 Å; after melt processing, the layers were partially re-aggregated. The length and orientation of the alkylammonium ions principally controlled the interlayer spacings within these aggregates. A finer degree of dispersive mixing of the clay in the polymerisation system was observed. The presence of modified clay in the polymerisation system led to branching, reduction of average molecular weight, increase in polydispersity, and to a bimodal molecular weight distribution of the PMMA. The glass–rubber transitions were observed around 120°C in the polymerisation system in comparison with 105°C for the melt intercalation materials and the PMMA resin. Moreover, PMMA extracted from the polymerisation composites had similarly elevated glass transition temperatures. The chain branching in the polymerisation system was the principal reason for the differences in the thermomechanical behaviour of the two composites.

Keywords: Clay; Composite; Relaxation; Poly(methyl methacrylate)

1. Introduction

Polymer/clay composites have been prepared through in-situ polymerisation of monomers within the galleries of modified clays [1] and through intercalation from solution [2]. It has been reported that several of these composites exhibited improved mechanical [3] and barrier properties [4], in comparison with the matrix polymer. Vaia et al. [5] presented a method for the melt intercalation of polymer chains. The process involves mixing a modified layered silicate with the polymer and heating to above the glass transition temperature and melting point, where appropriate, of the polymer. The materials that have been prepared through melt intercalation include polystyrene [6] and polypropylene [7] composites.

In a previous report by the authors [8], the preparation of poly(methyl methacrylate) (PMMA)/clay composites, through solution polymerisation of methyl methacrylate (MMA) in the presence of dodecylammonium and hexadecyltrimethylammonium-modified montmorillonite clay, was described. X-ray diffraction showed that the clay layers were separated by a distance greater than 80 Å in the powdered reaction products, as there were no reflections from the (001) plane of montmorillonite in the range 1–10° 2θ. This resulted from the large expansion of the clay aggregates during

---

* Corresponding author. Tel.: +662-246-1358-74, ext.: 1309; fax: +662-247-7050.

E-mail address: frrav@mahidol.ac.th (R.A. Venables).

PII: S0014-3057(00)00061-6

polymerisation. However, re-aggregation of the clay particles during subsequent melt processing was observed. After melt processing, the interlayer spacings in the clay aggregates were approximately the same as the lengths of the extended pre-intercalated alkylammonium ions, i.e. around 20 Å for dodecylammonium clay and 29 Å for the hexadecyltrimethylammonium clay. From this observation, it was suggested that the alkylammonium ions were fully extended and stood perpendicular to the internal clay surfaces, thereby controlling the interlayer spacings, with the PMMA chains occupying the remaining interlayer volume. Thus, the clay layers changed from the expanded arrangement created during solution polymerisation to a closer packed configuration during the melt processing.

In the work described herein, the PMMA/clay composites were prepared through direct melt intercalation during melt mixing. The microstructures and relaxation characteristics of these samples were compared with those in the solution-polymerised composites. Of particular interest were the thermomechanical properties and how they were affected by the composite preparation methods, the objective being to find the most suitable method of preparing PMMA/composites that gives an enhanced modulus at elevated temperatures.

2. Experimental

2.1. Materials

The hydroquinone inhibitor was extracted from the MMA monomer, from Fluka, with aqueous sodium hydroxide, then washed with distilled water, and dried over anhydrous sodium sulphate. Bentonite clay, containing a minimum of 90% montmorillonite, was from Colloid Environmental Technologies Co., Ltd. Dodecylamine was from Fluka and 2,2′-azo-bis(isobutyricnitrile) (AIBN) initiator was supplied by TPI Co., Ltd., Thailand.

2.2. Modification of clay

The clay (20 g), possessing a *d*-spacing of the (0 0 1) plane, d_{001}, of 12.9 Å, was dispersed in distilled water (600 ml) at 80°C. A solution of dodecylamine or hexadecyltrimethylammonium chloride (0.05 mol) and concentrated hydrochloric acid (4.8 ml) in distilled water (100 ml) was added; heating and stirring was continued for 1 h. The suspension was filtered, and the solid residue washed with hot distilled water until no chloride was left, as determined by using the silver nitrate test. The product was dried at 60°C for several days in a fan oven, then milled in a ball mill and subsequently dried at 60°C under vacuum for 24 h, yielding the dodecylammonium-modified clay or hexadecyltrimethylammonium clay; d_{001} of these clays were 17.9 and 19.7 Å, respectively.

2.3. Solution polymerisation

AIBN (0.1 g) was dissolved in the extracted MMA (10 g), followed by the addition of the modified clay (1, 2, 5, or 10 g) and distilled hexane (40 ml). For the highest clay contents, 100 ml of hexane was needed to disperse the clay. The reaction flask was suspended in a thermostated water bath at 68°C for 5 h, with a condenser fitted. The solid, powdered product was recovered from the reaction mixture by evaporation of the solvent, followed by drying under vacuum at 60°C.

2.4. Melt processing

Melt-intercalated composites were prepared by melt mixing the PMMA resin with the modified clay (10, 20, and 50 phr) in a Haake Rheocord 90 at 180°C for 10 min, with a rotor speed of 50 rpm. This procedure was repeated with the unmodified clay, for comparison. The products from the solution polymerisations were also melt fluxed to provide a processing history. All samples were compression moulded at 180°C to form plaques for characterisation.

2.5. Characterisation

The X-ray diffraction (WAXD) was carried out using wide angle a JEOL JDX-3530 diffractometer. The radiation source was operated at 30 kV and 30 mA; all but the CuK$_\alpha$ X-ray photons were filtered out of the beam. The scanning speed, step angle, and count time were 1.2° 2θ/min, 0.04° 2θ, and 2 s, respectively. For the scan range 1–10° 2θ, the divergence slit, receiving slit, and scattering slit were 0.5°, 0.1 mm, and 0.5°, respectively, whilst for the range 3–40° 2θ these values were 1°, 0.2 mm, and 1°, respectively. The precision of the *d*-spacings calculated from the X-ray data was assessed by measuring the *d*-spacing associated with a diffraction due to a biotite impurity in the clay at 10.2° 2θ as an internal standard. The mean *d*-spacing was 8.5 Å, standard deviation 0.08, and coefficient of variation 1%, based upon nine measurements. Transmission electron microscope (TEM) observations of sections were carried out with a JEOL JEM-100CX instrument. To assess the degree of dispersion of the clay particles in the TEM images, a line intersection method was employed. The frequency of the clay aggregate intersections with a line drawn along the micrograph, corresponding with the direction normal to the surfaces of the compression moulded plaque, was determined for each formulation. The results are given in the form of frequencies, expressed as the number of aggregate intersections with the line per μm. Dynamic mechanical analyses (DMA) were obtained with a

Polymer Laboratories DMTA mkII thermal analyser. Glass transition temperature, T_g, was determined from the maximum in the tanδ versus temperature scan. The PMMA was extracted from the compounds with tetrahydrofuran using a Soxhlet apparatus; the polymer was recovered through precipitation with methanol followed by drying. Differential scanning calorimetry (DSC) data were obtained with a Perkin Elmer DSC7 instrument. Samples were heated at 10°C/min to 180°C, cooled at 10°C/min to 50°C and finally heated at 10°C/min to 180°C. The data discussed herein were taken from the second heating phase of the cycle. T_g was determined from the mid-point of the step transition in the heat capacity versus temperature thermogram. Several replicate thermal analyses were carried out for each sample; the data reported are the mean values. ^{1}H and ^{13}C nuclear magnetic resonance (NMR) spectra were collected using a Bruker 300 MHz spectrometer employing $CDCl_3$ as the solvent. Gel permeation chromatography (GPC) was carried out using a Waters 150-CV Plus instrument at room temperature with tetrahydrofuran as the solvent and PMMA calibration standards.

3. Results and discussion

3.1. Clay expansion during composite preparation

Fig. 1 displays the representative X-ray diffraction traces for (a) samples prepared through melt intercalation, (b) polymerisation compounds after melt processing, and (c) reaction products from polymerisation before melt processing, each containing 20 phr of dodecylammonium clay; (d) is PMMA without clay. The abscissa are given in d-spacings calculated from the Bragg equation

$$d_{hkl} = \frac{n\lambda}{2\sin\theta}, \tag{1}$$

where $n = 1$, $\lambda = 1.542$ Å, and angle, θ. The X-ray traces for the unmodified clay filled PMMA were little different from the original unmodified clay, since the unmodified clay particles are simply incorporated into the polymer matrix in an agglomerated state, with no intercalation of the polymer. For both the melt processed polymerisation and melt-intercalation composites, a series of reflections exhibiting periodicity along the d-axis are present in the diffraction traces. These are the 0 0 l reflections for the (0 0 l) plane and indicate that the clay layers are at least partially arranged into aggregates that comprise regularly spaced layers. The average d_{001} for the melt-intercalation composites was 30.2 Å and changed little with clay content. The corresponding value for the melt processed polymerisation composites was 29.2 Å, and was independent of clay content. The gallery spacing, S_g, is the distance between the internal surfaces of neighbouring clay layers; it is calculated

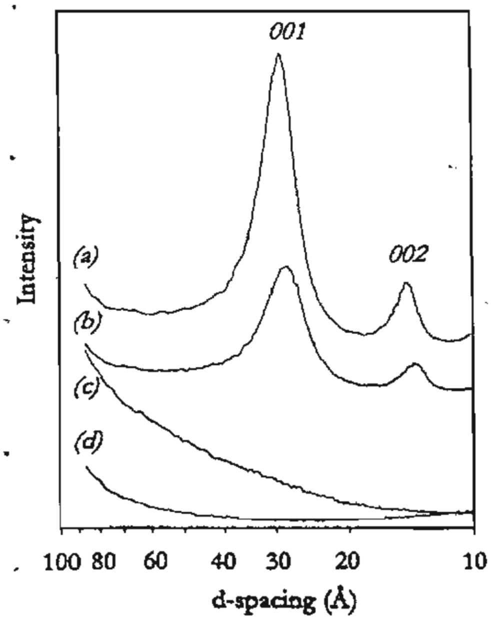

Fig. 1. WAXD traces of composites, containing 20 phr of dodecylammonium clay, prepared through (a) melt intercalation; (b) polymerisation (after melt processing); (c) polymerisation (powder reaction products before processing), and (d) PMMA synthesised in the absence of clay.

$$S_g = d_{001} - t, \tag{2}$$

where t is the van der Waal's thickness of the clay layer, that is 9.6 Å [9]. The gallery spacings are thus 20.6 and 19.6 Å for the intercalation and melt processed polymerisation composites, respectively. The length of an extended dodecylammonium ion is estimated to be 20.0 Å [9]; and hence, it is inferred that the extended ions stand perpendicular to the surface of the clay with the PMMA chains occupying the remaining space.

For the melt-intercalation composites, the preparation process may be described qualitatively by the following reasoning: in the dodecylammonium-modified clay, before composite preparation, the d_{001} was 17.9 Å, giving a corresponding interlayer spacing of 8.3 Å. This result suggests that the ions assume a bilayer arrangement [9], that is with one ion lying parallel to each of the internal surfaces of the clay. During melt mixing, the PMMA chains intercalate the clay interlayers, with the alkyl chains of the ions turning through 90° to become oriented perpendicular to the clay surface, thereby providing room to accommodate the PMMA. The favourable interactions between PMMA and the surface of the silicate sheets, and the gain in entropy of the alkyl chains as the interlayer spaces expand, permit an unfavourable loss in entropy of the polymer, due to its confinement between the silicate sheets, to be overcome [10,11]. Consequently, intercalation of the PMMA chains takes place during melt mixing. Further polymer intercalation does not occur, however, because once the alkyl chains are fully extended, no further entropy can be gained by the alkylammonium ions with continued layer expansion, and therefore, there is no driving force to overcome the associated loss in entropy as extra polymer is confined in the galleries.

This hypothesis was tested by melt intercalating PMMA into the galleries of a clay sample that had been modified with an ion possessing a different length from the dodecylammonium ions, namely hexadecyltrimethylammonium ions. The d_{001} of the composite was 39.7 Å, and hence, the gallery spacing was 30.1 Å. The estimated extended chain length of the hexadecyltrimethylammonium ion is 29.0 Å, and therefore, it is reasonable to conclude that the extended ions assume a perpendicular orientation to the inner surfaces of the clay, thereby playing a major role in determining the interlayer spacing.

The gallery spacings for all formulations are plotted versus the clay content as shown in Fig. 2. It can be seen that the melt intercalation samples have slightly higher spacings than the melt processed polymerisation materials. This result is obtained for every concentration of the clay, suggesting that the difference is reproducible, and hence significant relative to the estimated 1% error of the measurements. The origin may lie in the microstructure differences of the polymers, as discussed in Section 3.2.

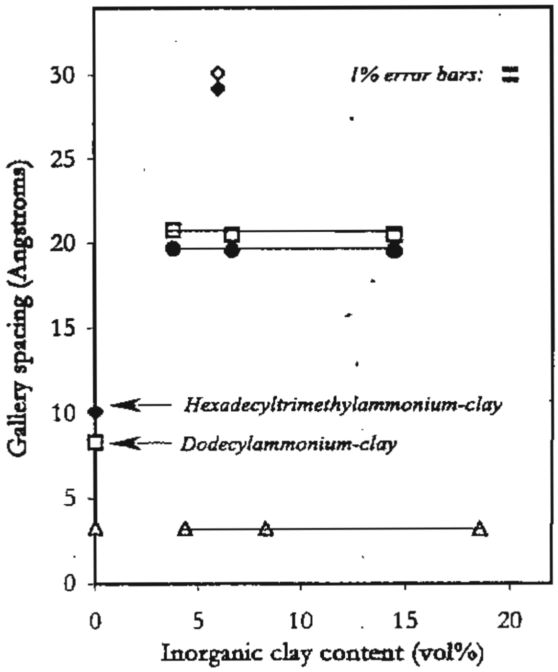

Fig. 2. Gallery spacings for all composites as a function of clay content: (Δ) PMMA/unmodified clay composites; (●) polymerisation composites containing dodecylammonium clay; (□) melt-intercalation composites containing dodecylammonium clay; (◆) polymerisation composites containing hexadecyltrimethylammonium clay, and (◇) melt-intercalation composites containing hexadecyltrimethylammonium clay.

3.2. Polymer microstructure

For both the polymerisation and melt-intercalation composites, all the PMMA could be extracted with tetrahydrofuran in a Soxhlet apparatus. Thus, in each composite, the polymer interacts with the clay through physical bonds that can be displaced through the formation of the tetrahydrofuran-clay specific interactions. Each extracted polymer was characterised through the GPC and NMR spectroscopy. The GPC data for the polymerisation system are displayed in Fig. 3; the melt-intercalation polymer was unchanged from the original resin. Polymerisation of MMA in the presence of higher loadings of modified clay resulted in the formation of polymers with reduced molecular weight and increased polydispersity, in comparison with the PMMA prepared under comparable conditions in the absence of clay. This may be due to the interference of active sites upon the clay surface with the free radical polymerisation; chain transfer to Lewis or Brönsted acid sites may take place.

SHOULD BE
-5
i.e. minus five

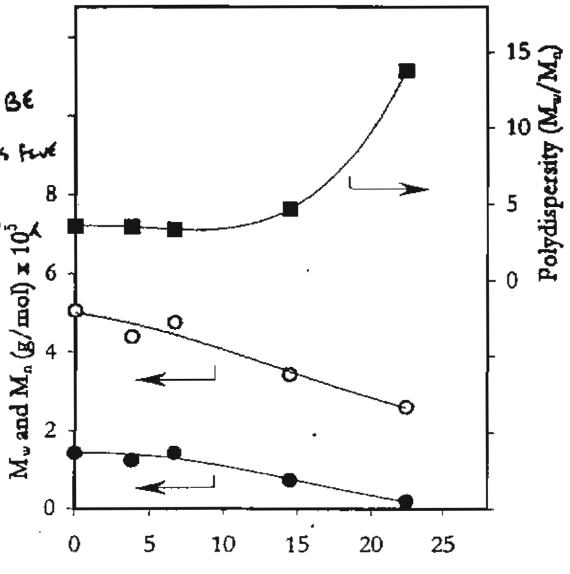

Fig. 3. GPC data for PMMA extracted from polymerisation composites: (O) weight average molecular weight, M_w; (●) number average molecular weight, M_n, and (■) polydispersity.

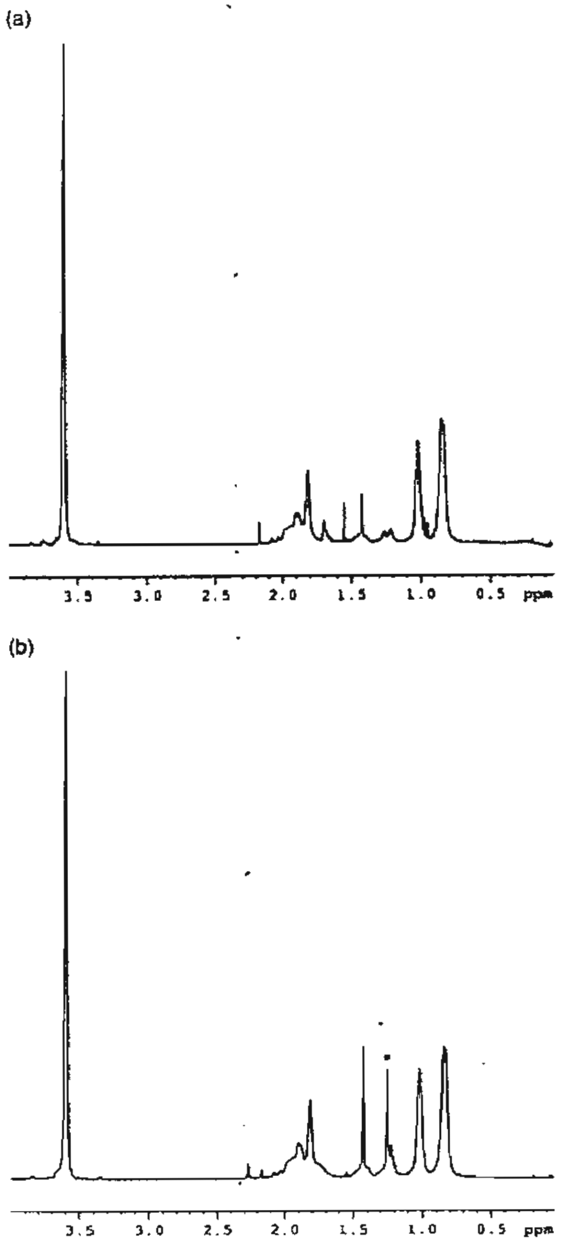

Fig. 4. ^{1}H-NMR spectra of (a) PMMA synthesised in the absence of clay and (b) PMMA extracted from a polymerisation composite containing 20 phr of dodecylammonium clay.

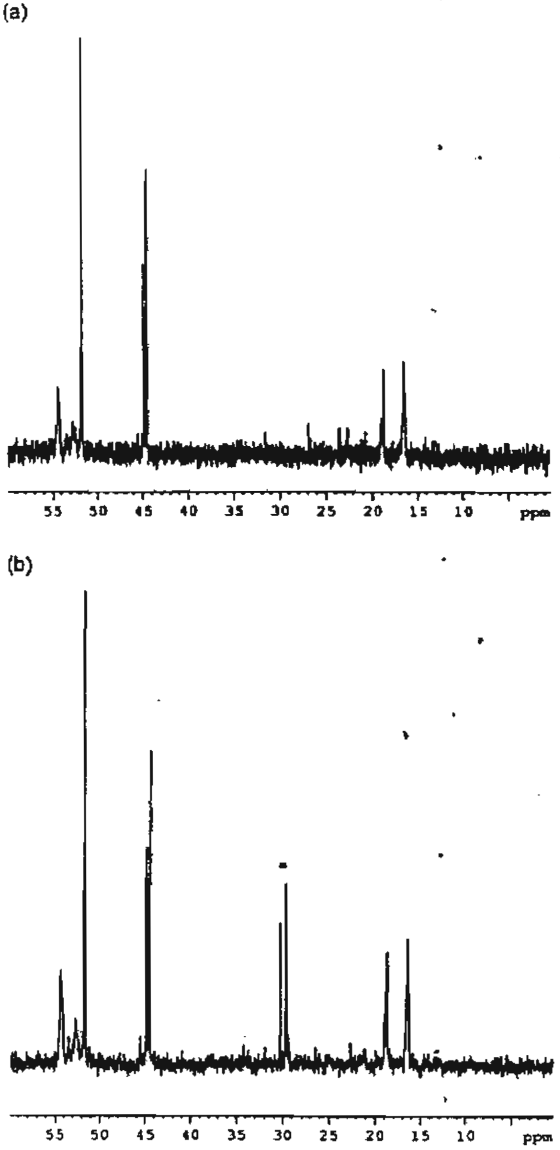

Fig. 5. ^{13}C-NMR spectra of (a) PMMA synthesised in the absence of clay and (b) PMMA extracted from a polymerisation composite containing 20 phr of dodecylammonium clay.

In Fig. 4 the ^{1}H-NMR spectrum of PMMA synthesised in the presence of modified clay is compared with the spectrum of PMMA prepared in the absence of clay; Fig. 5 shows the corresponding ^{13}C-NMR spectra. The resonances observed in the ^{1}H-NMR spectrum of PMMA prepared in the absence of clay may be assigned from previous studies [12]: OCH_3 at $\delta = 3.60$ ppm, CH_2 in the range $\delta = 2.50$ to 1.30 ppm, CH_3 at $\delta = 1.21$, 1.02, and 0.85 ppm, from isotactic, heterotactic, and syndiotactic triads, respectively. The PMMA synthesised in the presence of clay has an additional resonance at 1.25 ppm (marked with the symbol '■' in Fig. 4b); the area of this peak increased with increasing quantites of clay in the reaction vessel. Whilst this peak is in close proximity to the CH_3 resonance of the isotactic triads, it can be discounted as resulting from an increase in the fraction of isotacticity, since the splitting pattern of the CH_2 protons ~~are~~ not consistent with this result [12]. The ^{13}C- is

NMR spectrum of PMMA synthesised in the presence of clay has chemical shifts of 29.7 and 30.3 ppm, marked with the symbol '■' in Fig. 5b, which are not present in the spectrum of PMMA synthesised in the absence of clay. The ^{13}C-NMR and ^{1}H-NMR results are consistent with the formation of $\equiv$C–H structures, with the 29.7 and 30.3 ppm resonances being assigned to the tertiary carbon and the 1.25 ppm resonance to the methine proton. These results suggest that the polymer prepared in the presence of clay contains branch points, and hence, it is concluded that this is promoted by the active involvement of the clay surface during polymerisation.

In the GPC chromatograms of PMMA extracted from the composites containing 20 phr or more of clay, as exemplified in Fig. 6, it is evident that there is a bimodal distribution of molecular weights. This may result from the heterogeneous conditions of the polymerisations carried out in the presence of clay. Reactions taking place in close proximity of the clay surface may readily interact with the active sites of the clay leading to the formation of the lower molecular weight and more highly branched polymer. Both factors lead to reduced coil dimensions, and therefore longer retention times in the GPC column. Polymerisations progressing at some distance from the clay have lower probabilities of being affected, and hence, a higher molecular weight fraction may be formed. It is possible that the more highly branched polymer, with lower molecular weight, formed near the clay surfaces locates in the clay galleries. It was noted previously that the clay gallery spacings were always smaller in the polymerisation system than in the intercalation system. The observation may be related to the altered microstructure of the PMMA when prepared in the presence of clay. Branching results in reduced coil dimensions, changes in the conformations of the polymer chains, and to an increase in the number of polymer chain ends in comparison with a linear polymer of the same molecular weight [13]. Thus, the free energy of interaction between the PMMA, alkylammonium ions, and the clay is affected resulting in the modification of the clay aggregate structure.

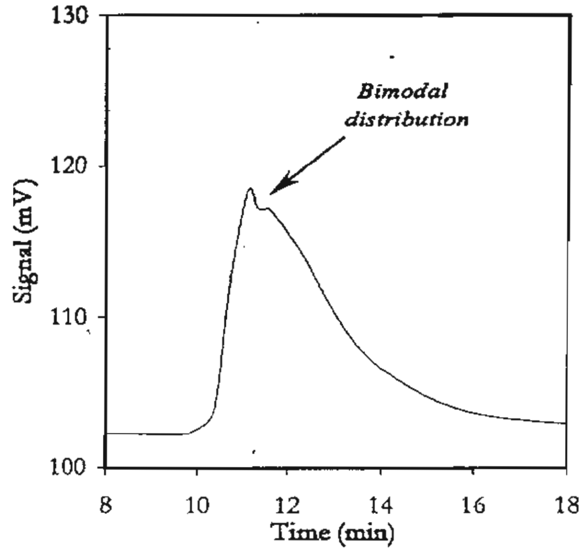

Fig. 6. GPC chromatogram of PMMA extracted from the polymerisation composite containing 50 phr of dodecylammonium clay.

3.3. Clay aggregate dispersion

The appearances of the polymerisation and melt-intercalation composites to the naked eye were similar, in that both were transparent. It may be inferred from the observation that the clay aggregates in these materials are small relative to the wavelengths of visible light and hence, little diffraction occurs. Conversely, the compounds containing unmodified clay were opaque, indicating the presence of large agglomerates that scatter light. The SEM micrographs shown in Fig. 7 confirm the presence of large agglomerates in the composites prepared with the unmodified clay, in comparison with the finer textures seen for the melt-processed polymerisation and melt-intercalation composites. The alkylammonium ions reduce the attractive forces between the clay layers and enable the polymer or monomer to intercalate into the clay galleries thereby aiding the dispersion of the clay. The average thickness of the clay crystal aggregates perpendicular to the (0 0 1) plane, L_c, was calculated using the Scherrer equation

$$L_c = \frac{k\lambda}{\beta_{001}\cos\theta}, \tag{3}$$

where $k = 1$ and β_{001} is the width, in radians, at half maximum intensity of the 0 0 1 reflection.

The average number of layers in each aggregate, N_c, was calculated:

$$N_c = \left(\frac{L_c}{d_{001}}\right) + 1. \tag{4}$$

L_c and N_c values for the two types of composite are plotted as functions of the clay content in Fig. 8. It is inferred from the data that in the polymerisation system, for the two lowest clay contents, the clay is dispersed into a larger number of aggregates each comprising fewer silicate sheets than in the melt-intercalation composites. At the highest clay content, however, the X-ray analysis reveals little difference between the two types of composite. The peak width, β_{001}, may be increased due to the disorder in the crystals in addition to the influence of the finite crystallite size, and hence, the calculated L_c may decrease. The TEM measurements plotted in Fig. 9 show that, for a given clay content, there is a larger

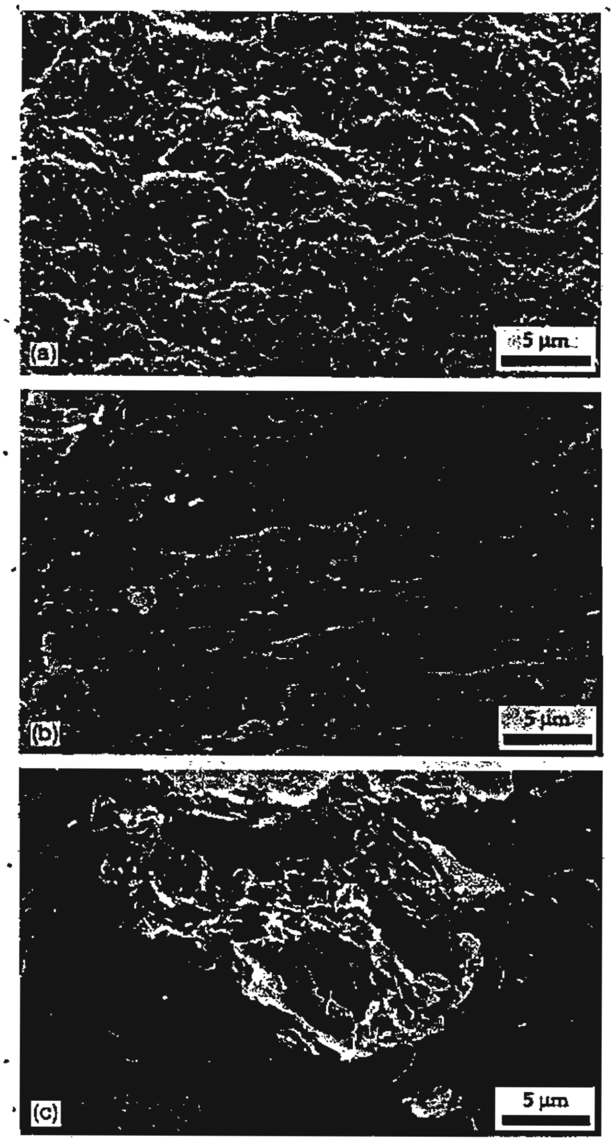

Fig. 7. SEM micrographs of fracture surfaces: (a) melt processed polymerisation PMMA/dodecylammonium clay composite; (b) PMMA/dodecylammonium clay melt-intercalation composite, and (c) unmodified clay filled PMMA; content is 10 phr in each sample.

clay

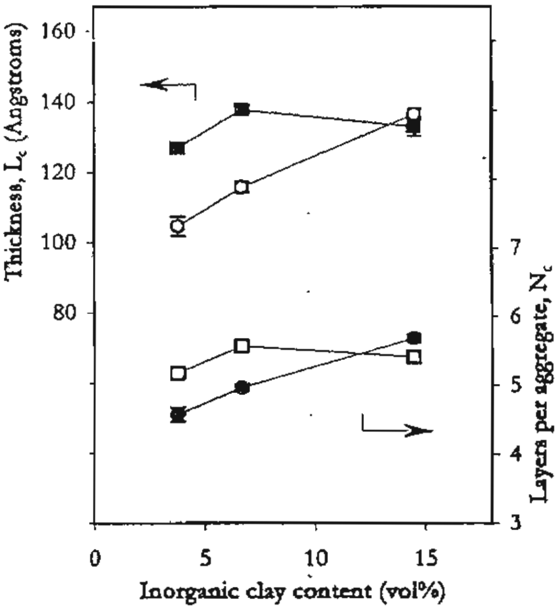

Fig. 8. Average crystallite thickness, L_c, in the (○) melt processed polymerisation and (■) melt intercalation systems containing dodecylammonium clay; average number of clay layers per aggregate, N_c, versus clay content in the same (●) polymerisation and (□) melt-intercalation composites.

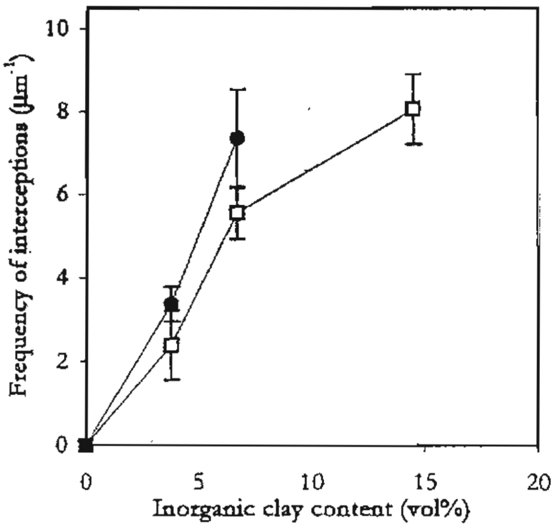

Fig. 9. Plot of number of clay aggregate-line intersections per micron for: (□) melt-intercalation composites and (●) melt processed polymerisation composites, both containing dodecylammonium clay.

number of clay aggregates in the polymerisation composites than in the intercalation composite; i.e. the aggregates are smaller in the former material. This confirms that the increases in β_{001} at least partly reflect reductions in the crystallite thickness. Examples of the TEM micrographs from which the data in Fig. 9 were obtained are displayed in Fig. 10. The clay layers are oriented on one plane, that is, with the basal surfaces, and hence the (0 0 1) plane, parallel to the platens of the compression press. Moreover, the 1 0 0 reflection of the quartz in the clay was not seen in the X-ray diffraction traces of the moulded samples, indicating its perpen-

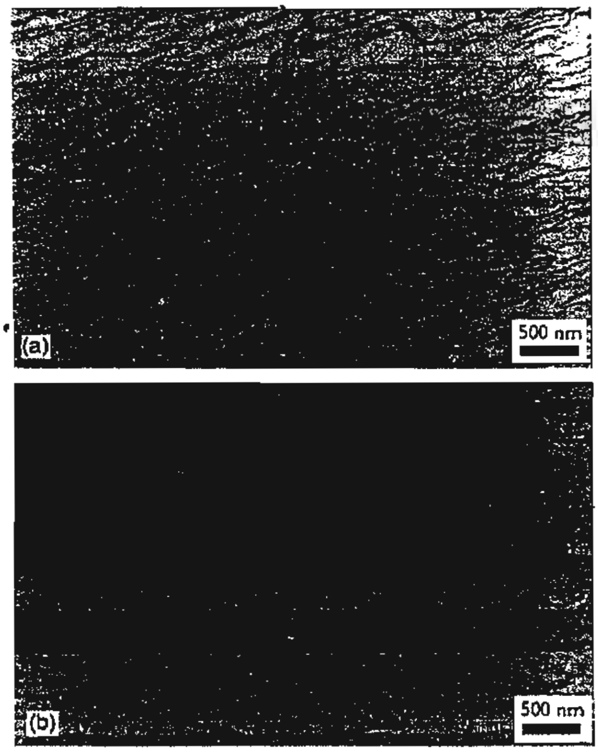

Fig. 10. TEM micrographs of PMMA/dodecylammonium clay composites, containing 20 phr of clay: (a) melt processed polymerisation and (b) melt-intercalation composites.

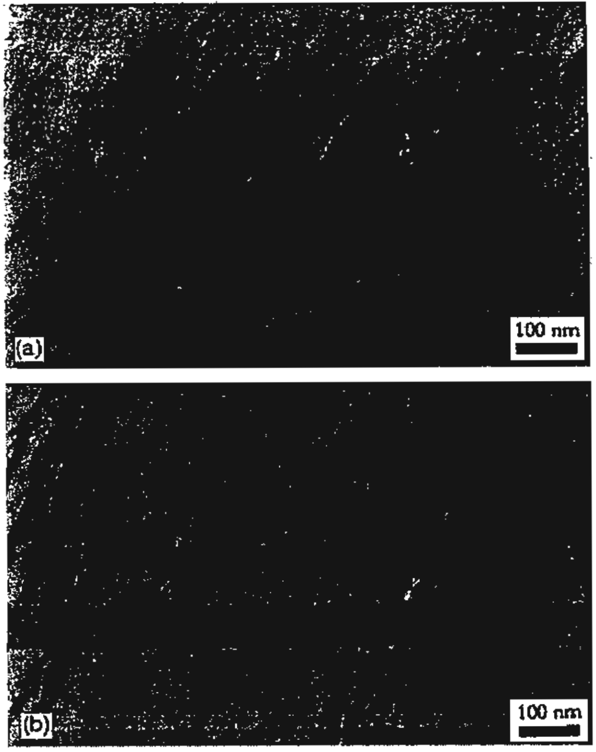

Fig. 11. TEM micrographs of PMMA/dodecylammonium clay composites: (a) melt processed polymerisation and (b) melt intercalation samples; clay content is 50 phr in both.

dicular orientation to the platens. The TEM micrographs of the composites containing the highest clay content, shown in Fig. 11, reveal differences in the arrangement of the clay aggregates in the two composites. In the polymerisation composite, the aggregates form an almost continuous pattern, with a large amount of connectivity, overlap, and misalignment within the aggregates, making differentiation of individual aggregates unclear. The line intersection method was uncertain for this micrograph and consequently no data are given in Fig. 9 for the sample. The melt-intercalation composite has more regular and clearly defined aggregates.

The differences in the polymerisation and melt-intercalation composite structures originate from the conditions during sample preparation. The polymerisation reactions took place in a dispersion of modified clay in MMA dissolved in hexane in which the monomer was able to penetrate the clay galleries causing the clay to swell to a separation beyond the detection limit of the X-ray diffraction analysis; i.e. greater than 80 Å. As the molecular weight of the polymer increased during polymerisation, the chains precipitated from the solution became trapped between the silicate sheets, thereby fixing their separation. However, it is probable that some long-range order between the clay sheets was maintained. During subsequent melt processing, some of the PMMA chains moved out from between the layers and the silicate sheets aggregated into more thermodynamically favoured arrangements. The silicate sheets may not have returned wholly to their original positions, with sheet misalignment resultant in the newly formed aggregates. In the melt intercalated sample, the aggregates appear to be well separated from one another, in discrete aggregates. During melt intercalation, the PMMA intercalates the clay crystal aggregates causing them to expand in the (0 0 1) direction, i.e. normal to the (0 0 1) plane, without causing the layers to loose the vertical alignment of the crystal lamellae. Consequently, more of the original order is maintained in the melt-intercalation composites.

d/
a/

SHOULD BE SQUARE BRACKET FOR DIRECTION i.e. [001]

3.4. Relaxation characteristics

The plots of T_g, determined from DMA, against dodecylammonium clay content are shown in Fig. 12. Typical storage modulus curves are shown in Fig. 13. T_g values of the melt-intercalation composites were close to that of the unfilled PMMA, i.e. around 105°C. The

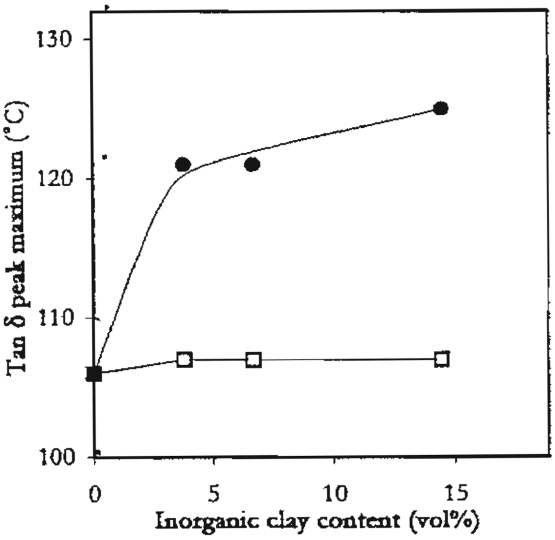

Fig. 12. Temperature of tanδ maximum versus inorganic clay content: (☐) melt intercalation and (●) melt processed polymerisation composites, containing dodecylammonium clay.

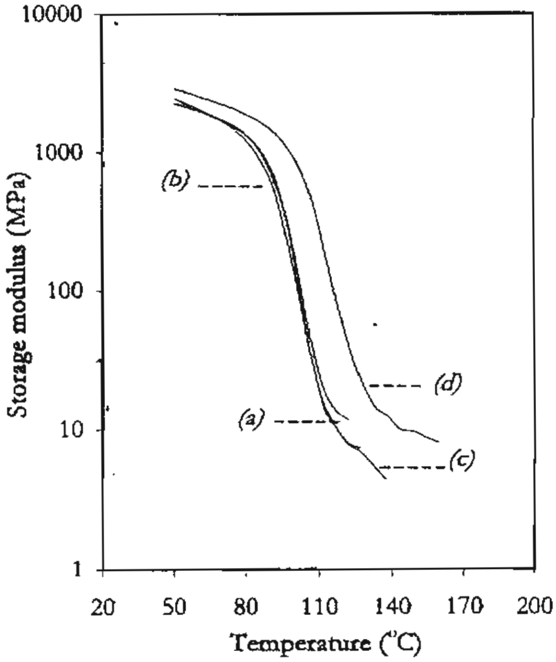

Fig. 13. Storage modulus versus temperature for (a) unfilled PMMA and (b) PMMA with unmodified clay. Curve (c) and (d) are from the melt intercalation and melt processed polymerisation composites, respectively, containing 10 phr of dodecylammonium clay.

polymerisation composites exhibited pronounced increases in T_g, typically of 20°C, in comparison with pure PMMA that was slightly affected by the clay concentration, although the rate of increase in T_g decreased with increasing clay contents. Moreover, the storage moduli of the solution-polymerised composites were substantially greater, at every temperature, in comparison with the other formulations. T_g, determined through DSC analyses, of the polymers extracted from the composites showed essentially the same result, although the values obtained from DSC were typically 5°C lower than those obtained from DMA mainly due to the static versus dynamic nature of the DSC and DMA analyses. Thus, changes in T_g may be traced to structural differences in the polymer. Modulus may be affected to some extent by the greater dispersion of the clay in the polymerisation composites due to the hydrodynamic effects. The NMR results showed that the PMMA prepared in the presence of clay was branched. The chain structure affects T_g in PMMA markedly, e.g. for the isotactic form $T_g = 45$°C, for syndiotactic $T_g = 115$°C, and for statistical polymers prepared through free radical polymerisation $T_g = 99$°C [14]. Moreover, Krigas et al. [15] observed an increase in T_g with increasing branch contents of model polyethylenes. It is likely that the chain branching is the cause in the modified relaxation characteristics of the PMMA in the polymerisation composites. The effect of branching ,may be more pronounced in PMMA due to the bulkiness of the branch points that restricts the main chain relaxation in comparison with the less sterically hindered polyethylene. From the results of Cowie [16], changes in the molecular weight over the range found in this work are not expected to alter T_g.

Vaia et al. [5] observed that whilst the main chain relaxation of the intercalated polystyrene in montmorillonite composites was suppressed, a transition due to the unintercalated bulk polymer was observed at the same temperature as the glass transition of the unfilled polymer resin. For the intercalated polymer, the relaxation process is limited by the restrictions imposed upon the chains through their confinement between the clay layers.

The available free volume may be insufficient to permit co-operative jump processes [17], with the consequence that the relaxation of the intercalated polymer is suppressed, at least within the time and temperature conditions of the analysis. The experimentally observed relaxations in this work originate from the polymer in the bulk.

4. Conclusions

1. Montmorillonite clay modified with dodecylammonium and hexadecyltrimethylammonium ions can be intercalated through melt mixing with PMMA.

2. The length and orientation of the extended alkylammonium ions principally control the interlayer spacings of the clay in both the melt intercalation and the melt processed polymerisation composites.
3. The clay aggregates in the melt processed polymerisation composites are more finely dispersed and are more misaligned than in the melt intercalation composites.
4. PMMA synthesised in the presence of the clay was branched and this led to an increase in the glass transition temperature of the polymer and the storage moduli of the polymerisation composites in comparison with the melt intercalation samples.

Acknowledgements

The authors would like to thank the Thailand Research Fund (TRF), for their support of this work, the National Metal and Materials Technology Centre (MTEC) for the use of the X-ray powder diffractometer, Siam Cement Co., Ltd., for donation of the clay, TPI Co., Ltd., for the donation of the AIBN, Tsuneo Chiba for the TEM work, and Prof. Ian Harrison for his comments.

References

[1] Messersmith PB, Giannelis EP. J Polym Sci A: Polym Chem 1995;33:1047.
[2] Giannelis EP. Adv Mater 1996;8(1):29.
[3] Lee DC, Jang LW. J Appl Polym Sci 1996;61:1117.
[4] Yano K, Usuki A, Okada A. J Polym Sci A: Polym Chem 1997;35:2289.
[5] Vaia RA, Ishii H, Giannelis EP. Chem Mat 1993;5:1694.
[6] Vaia RA, Jandt KD, Kramer EJ, Giannelis EP. Macromolecules 1995;28:8080.
[7] Hasegawa N, Kawasumi M, Kato M, Usuki A, Okada A. J Appl Polym Sci 1998;67:87.
[8] Tabtiang A, Lumlong S, Venables RA. Polym Plast Tech Eng 2000;39(2):293.
[9] Lan T, Kaviratna KD, Pinnavaia TJ. Chem Mater 1995;7:2144.
[10] Vaia RA, Giannelis EP. Macromolecules 1997;30:8990.
[11] Vaia RA, Giannelis EP. Macromolecules 1997;30:8000.
[12] Cowie JMG. In: Polymers: chemistry and physics of modern materials, 2nd ed. London: Blackie, 1991. p. 222.
[13] Balke ST. In: Barth HG, Mays JM, editors. Modern methods of polymer characterisation. New York: Wiley-Interscience, 1991. p. 86.
[14] Brydson JA. In: Plastics materials, 6th ed. Oxford: Butterworth-Heinemann, 1995. p. 62.
[15] Krigas TM, Carella JM, Struglinski MJ, Crist B, Graessley WW. J Polym Sci: Polym Phys Ed 1985;23:509.
[16] Cowie JMG. In: Polymers: chemistry and physics of modern materials. 2nd ed. London: Blackie, 1991. p. 270.
[17] Eisele U. In: Polymer physics. Berlin: Springer, 1990.